ACS Catalysis

pubs.acs.org/acscatalysis Research Article

1,4-Arylalkylation of Butadiene with Aryl Bromides and Amino Acids Enabled by Photo-Induced Chiral Aldehyde/Palladium Catalysis

Jian-Hua Liu,[⊥] Lei Xu,[⊥] Wei Wen, Zhu-Lian Wu, Tian Cai, Yan-Min Huang,* Yu Lan,* and Qi-Xiang Guo*

Cite This: *ACS Catal.* 2025, 15, 15734−15744 Read Online

ACCESS | Metrics & More | Article Recommendations | Supporting Information

ABSTRACT: Butadiene is one of the most important chemical feedstocks used for the construction of value-added molecules. However, much of the existing endeavors have primarily focused on the achiral synthesis. Alternatively, although the aryl radical-involved transformations have been extensively disclosed, the corresponding catalytic asymmetric methodologies remain exceedingly rare. In this study, we present a highly efficient three-component asymmetric 1,4-arylalkylation of butadiene utilizing readily available aryl bromides and NH_2-unprotected amino acid esters. This process is facilitated by photoinduced chiral aldehyde/palladium combined catalysis. A diverse array of chiral non-proteinogenic α,α-disubstituted α-amino acid esters with unique structures is generated with 35−81% yields and 71−98% ee values. The resulting products can be easily converted to other structurally diverse α-amino acids. Density functional theory (DFT) calculations indicate that the final enantioselectivity is governed by a synergistic reaction model that encompasses noncovalent interactions between Pd···Br···Zn as well as strong C−H···Br and $\pi\cdots\pi$ dispersion interactions.

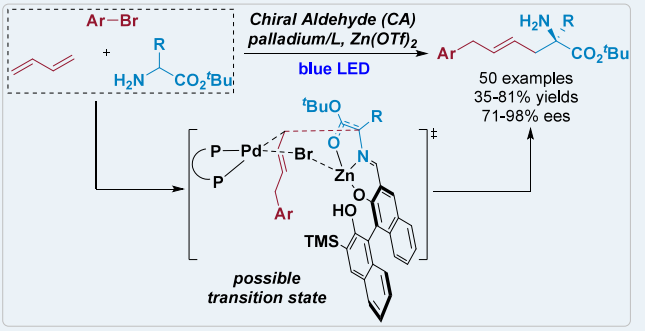

KEYWORDS: *butadiene, aryl radical, chiral aldehyde catalysis, palladium catalysis, chiral amino acid*

Downloaded via MPI CHEMICAL ENERGY CONVERSION on August 27, 2025 at 11:53:40 (UTC).
See https://pubs.acs.org/sharingguidelines for options on how to legitimately share published articles.

INTRODUCTION

Selectively converting chemical feedstocks into value-added molecules is a critical endeavor for synthetic chemists. In this context, the functionalization of butadiene—a fundamental chemical feedstock with an annual production of 1.3×10^7 tons, has emerged as one of the most dynamic research areas.[1−4] However, much of the existing research has concentrated on the synthesis of achiral molecules via polymerization,[5−9] hydrofunctionalization or bifunctionalization,[10−22] and the catalytic asymmetric modification of butadiene is extremely scarce (Figure 1a). A groundbreaking study on the use of butadiene in asymmetric catalysis was reported by Krische et al. in 2012.[23] They successfully achieved an asymmetric hydroalkylation reaction between butadiene and primary alcohols via Ru−H catalysis. Subsequently, Buchwald et al. unveiled a highly efficient catalytic asymmetric reductive addition of butadiene to ketones.[24] In 2022, Luo's group accomplished catalytic asymmetric 1,4-hydroalkylation or telomerization reactions involving butadiene by varying both the palladium source and phosphine ligand used.[25] In the same year, Zi and colleagues achieved an elegant catalytic asymmetric 1,4-bialkylation process utilizing tertiary alkyl bromides along with N-protected amino acid esters as reactants.[26] Besides these, Zhang,[27] Huang[28] and Yin[29] each disclosed their findings on catalytic asymmetric 1,2-bifunctionalization of butadiene. Most recently, Chen's group disclosed a nickel-catalyzed asymmetric 1,3-cyclotelomerization of butadiene that resulted in optically active [5,5] fused bicyclic compounds with commendable yields and excellent enantioselectivities.[30] Undoubtedly, further advancing catalytic asymmetric methodologies for modifying butadiene represents a significant contribution to this field.

On the other, as one of the most important aryl species, aryl radicals have been successfully used in the arylation of small organic molecules as well as complex natural products, pharmaceuticals, and materials.[31] However, most studies have primarily focused on constructing achiral target molecules;[32−35] only a limited number of examples have been realized with enantioselectivity (Figure 1b).[29,36] Recently, Ritter and collaborators described a highly efficient 1,4-aminoarylation of butadiene utilizing aryl halides and amines (Figure 1c).[37] In this process, the generation of an aryl radical, an allyl radical, and an π-allyl palladium species occurs

Received: July 15, 2025
Revised: August 19, 2025
Accepted: August 20, 2025

© XXXX American Chemical Society

https://doi.org/10.1021/acscatal.5c02967
ACS Catal. 2025, 15, 15734−15744

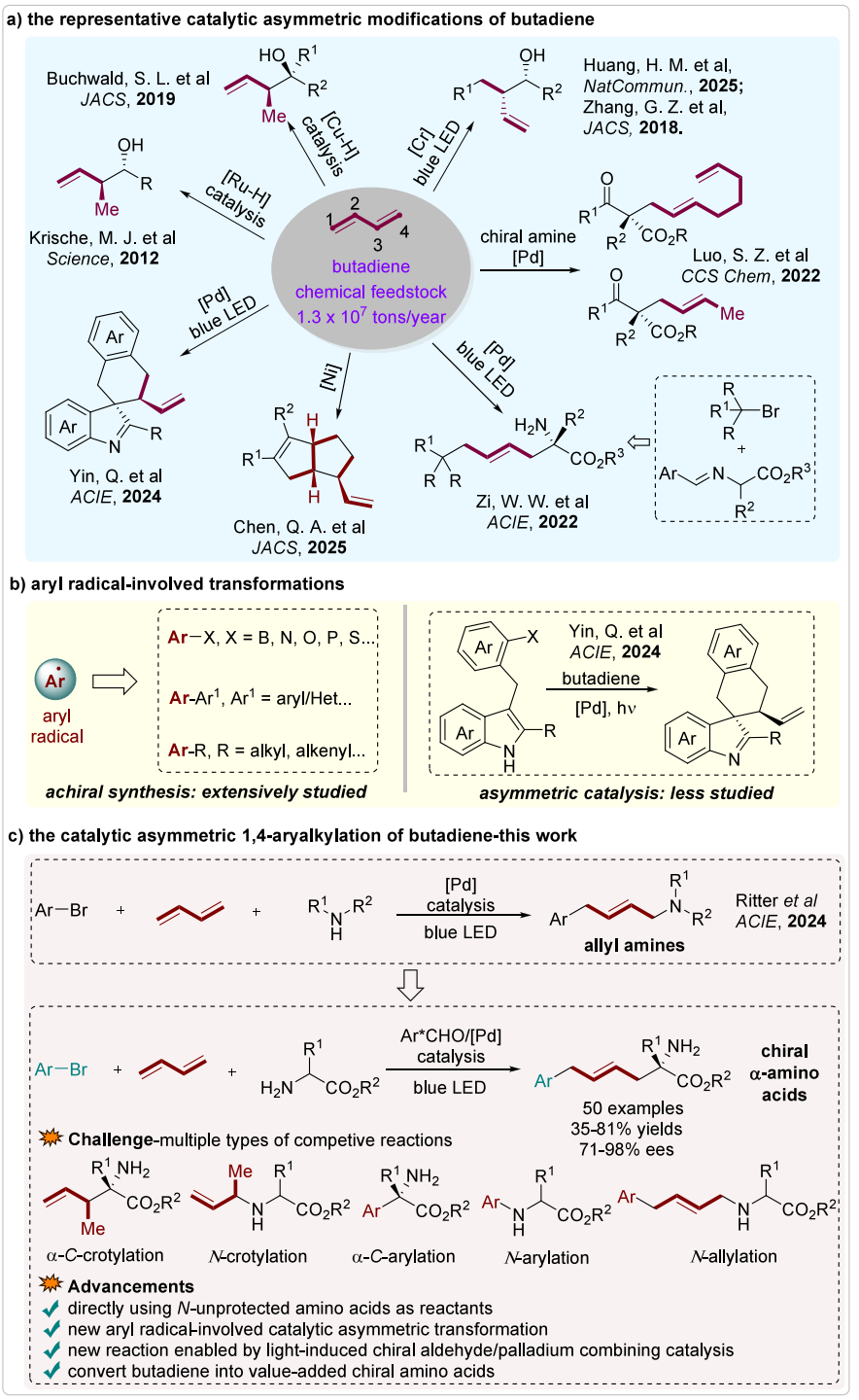

Figure 1. Research background and reaction design. a) Representative butadiene-involved asymmetric reactions. b) Aryl radical-involved transformations. c) Reaction design of this work.

successively before the *N*-allylation reaction takes place to yield the final product. In light of the extensively explored catalytic asymmetric allylation reactions via π-allyl palladium species, the generation of this type of species from aryl radical and butadiene offers promising prospects for further development in asymmetric transformations within the realm of aryl radical chemistry. However, to our knowledge, only Yin and colleagues have documented an asymmetric 1,2-arylalkylation of butadiene initiated by an aryl radical species.[29] The exploration of novel aryl radical-involved asymmetric arylation reactions remains largely uncharted territory.

Inspired by Ritter's findings[37] and building upon previous research concerning the chiral aldehyde/palladium-catalyzed α-C-allylation of NH_2-unprotected amino acid esters with various π-allyl palladium species,[38−42] we proposed that the active π-allyl palladium species generated from aryl bromides and butadiene under light-induced palladium catalysis could be enantioselectively trapped by the α-carbon anion of NH_2-unprotected amino acid esters through chiral aldehyde catalysis

https://doi.org/10.1021/acscatal.5c02967
ACS Catal. 2025, 15, 15734−15744

Table 1. Optimization of Reaction Conditions

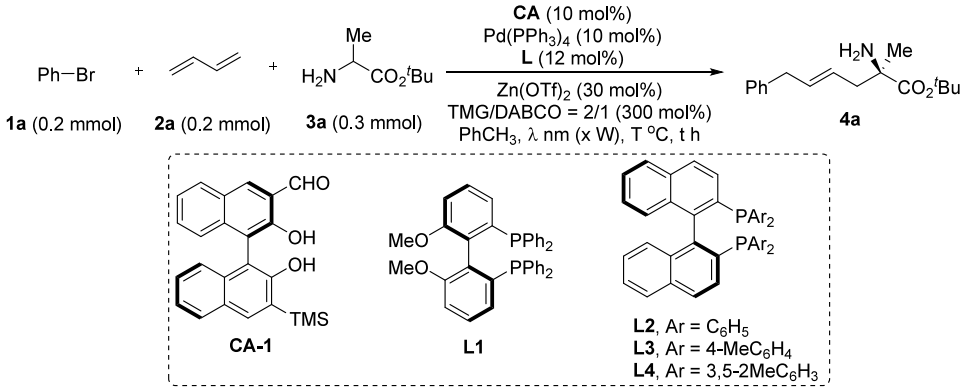

entry	CA	L	λ/x/T/t	y (%)[a]	ee (%)[b]
1	CA-1	L1	460/20/10/12	45	90
2	*ent*-CA-1	L1	460/20/10/12	22	48
3	CA-1	L2	460/20/10/12	35	90
4	*ent*-CA-1	L2	460/20/10/12	27	54
5	CA-1	L3	460/20/10/12	46	92
6	*ent*-CA-1	L3	460/20/10/12	24	40
7	CA-1	L4	460/20/10/12	39	90
8	*ent*-CA-1	L4	460/20/10/12	19	34
9[c]	CA-1	L3	460/20/10/12	56	90
10[c]	CA-1	L3	460/20/10/24	61	88
11[c]	CA-1	L3	450/40/30/12	68	90
12[c]	CA-1	L3	450/40/30/24	73	92
13[c,d]	CA-1	L3	450/40/30/24	80	92

[a]yield of isolated product. [b]determined by chiral HPLC. [c]with 0.4 mmol **1a**, 0.4 mmol **2a** and 0.2 mmol **3a**. [d]with using **2a** (20 wt % in toluene) as reactant.

(Figure 1c). Consequently, this asymmetric 1,4-bifunctionalization of butadiene is anticipated to be achieved for the construction of chiral nonproteinogenic amino acid derivatives.[43−47] However, the usage of N-unprotected amino acid esters would present various challenges for this reaction. Typically, the *α*-*C* or *N*-crotylation,[38] *α*-*C* or *N*-arylation,[48,49] and the *N*-allylation[50] would be the potential side products in this reaction. Controlling this three-component reaction that takes place via a Heck addition/allylation sequence is the key issue to suppress those undesired reactions.

RESULTS AND DISCUSSION

Reaction Condition Optimization. The phenyl bromide **1a**, butadiene **2a** (2 M in THF), and *tert*-butyl alaninate **3a** were selected as model reactants. To our satisfaction, under the irradiation of a blue LED (460 nm, 20 W), the catalytic system comprising chiral aldehyde **CA-1**, palladium $Pd(PPh_3)_4$, and Lewis acid $Zn(OTf)_2$ efficiently promoted this three-component reaction, yielding desired allylation product **4a** in 45% yield with an enantiomeric excess (ee) of 90%. Subsequently, several reaction conditions were optimized systematically. Chiral ligand screening revealed that the combination of chiral aldehydes **CA-1** and **L3** slightly enhanced both the yield and enantioselectivity of product **4a** (Table 1, entry 5). The *S*-conformation of ligands **L1**-**L4** was found to be compatible with the *R*-conformation of chiral aldehyde **CA-1**. When **CA-1** was substituted with its enantiomer ***ent*-CA-1**, there was a significant decrease in both yield and enantioselectivity for product **4a** (Table 1, entries 2, 4, 6 and 8). By extending the reaction time to a total of 24 h, we achieved an increased yield for product **4a** (Table 1, entry 10). Further optimization involved careful adjustments to the wavelength and power output of the LED light source as well as variations in reaction temperature. Notably favorable results were obtained when conducting this reaction under irradiation with a 450 nm, 40 W LED and at 30 °C, resulting in a yield reaching 73% with an ee value of 92% (Table 1, entry 12). The solvent of reactant **2a** exhibited little impact on the yield. With the utilization of reactant **2a** in toluene, the yield of **4a** was further improved to 80% (Table 1, entry 13). Based on these results, the optimal reaction conditions were determined.

Substrate Scope. With the optimal reaction conditions established, we proceeded to investigate the functional group tolerance of aryl bromides and amino acid esters (Figure 2). First, we examined the functional group tolerance of phenyl bromides. The results indicated that phenyl bromides bearing alkyl or aryl substituents could react smoothly with **2a** and **3a**, yielding the corresponding products **4b**-**4f** in high yields and excellent enantioselectivities. Additionally, phenyl bromides containing fluorine atoms also served as effective reaction partners with **2a** and **3a**, resulting in products **4g**-**4j** with yields ranging from 53% to 74% and ee values between 95% and 98%. Other heteroatom-containing functional groups such as trimethylsilyl (TMS), amino, amide, ether, ester, thioether, and boryl demonstrated good tolerance in this reaction. All corresponding aryl bromides produced products **4k**-**4u** with yields varying from 51% to 75% and ee values spanning from 71% to 98%. Subsequently, we investigated the functional group tolerance of heterocyclic aryl compounds. The findings revealed that aryl bromides containing furan, thiophene,

https://doi.org/10.1021/acscatal.5c02967
ACS Catal. 2025, 15, 15734−15744

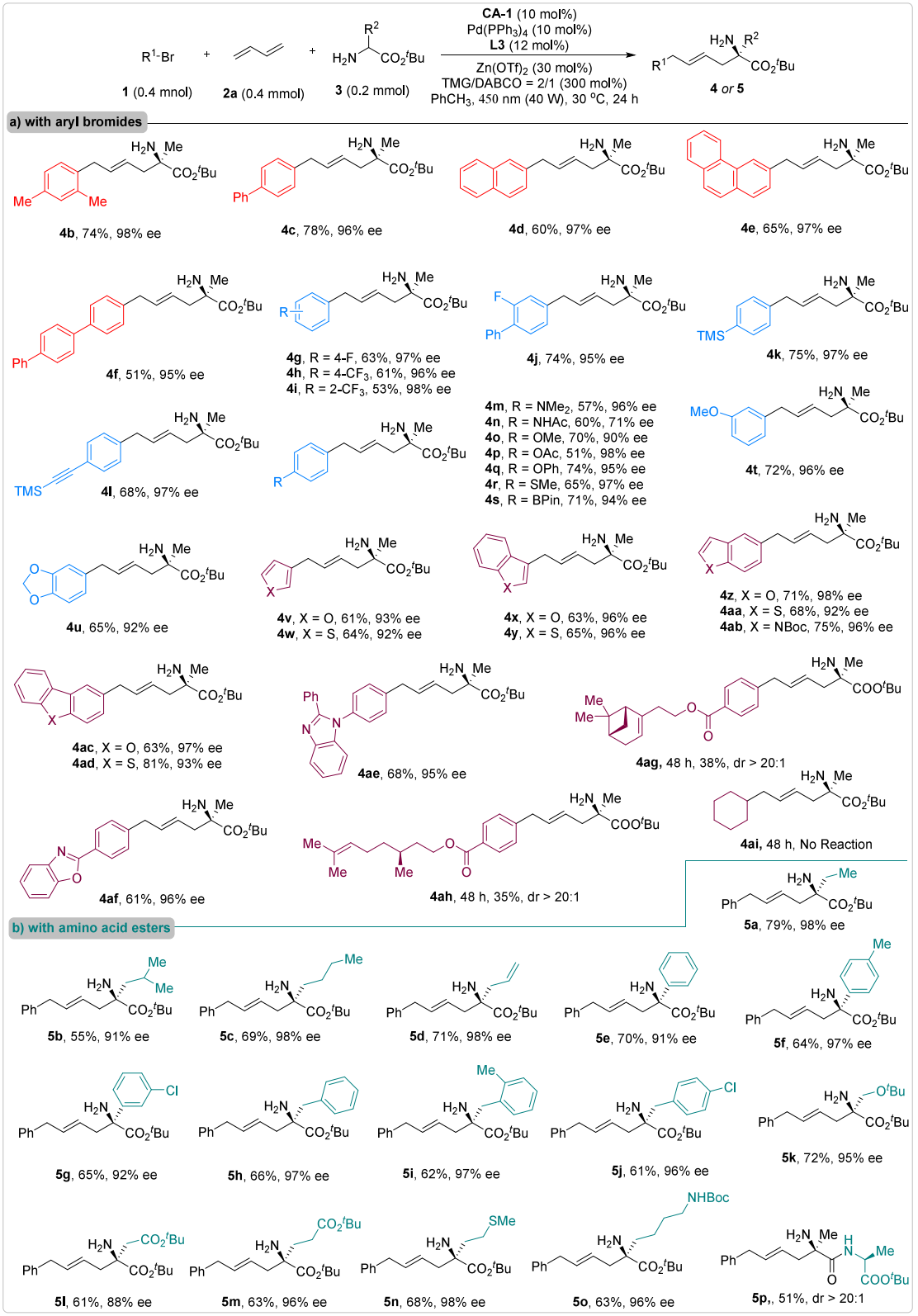
CA-1 (10 mol%)
Pd(PPh3)4 (10 mol%)
L3 (12 mol%)
Zn(OTf)2 (30 mol%)
TMG/DABCO = 2/1 (300 mol%)
PhCH3, 450 nm (40 W), 30 °C, 24 h
1 (0.4 mnol)
2a (0.4 mmol)
3 (0.2 mmol)
4 or 5
a) with aryl bromides
4b, 74%, 98% ee
4c, 78%, 96% ee
4d, 60%, 97% ee
4e, 65%, 97% ee
4f, 51%, 95% ee
4g, R = 4-F, 63%, 97% ee
4h, R = 4-CF3, 61%, 96% ee
4i, R = 2-CF3, 53%, 98% ee
4j, 74%, 95% ee
4k, 75%, 97% ee
4l, 68%, 97% ee
4m, R = NMe2, 57%, 96% ee
4n, R = NHAc, 60%, 71% ee
4o, R = OMe, 70%, 90% ee
4p, R = OAc, 51%, 98% ee
4q, R = OPh, 74%, 95% ee
4r, R = SMe, 65%, 97% ee
4s, R = BPin, 71%, 94% ee
4t, 72%, 96% ee
4u, 65%, 92% ee
4v, X = O, 61%, 93% ee
4w, X = S, 64%, 92% ee
4x, X = O, 63%, 96% ee
4y, X = S, 65%, 96% ee
4z, X = O, 71%, 98% ee
4aa, X = S, 68%, 92% ee
4ab, X = NBoc, 75%, 96% ee
4ac, X = O, 63%, 97% ee
4ad, X = S, 81%, 93% ee
4ae, 68%, 95% ee
4ag, 48 h, 38%, dr > 20:1
4af, 61%, 96% ee
4ah, 48 h, 35%, dr > 20:1
4ai, 48 h, No Reaction
b) with amino acid esters
5a, 79%, 98% ee
5b, 55%, 91% ee
5c, 69%, 98% ee
5d, 71%, 98% ee
5e, 70%, 91% ee
5f, 64%, 97% ee
5g, 65%, 92% ee
5h, 66%, 97% ee
5i, 62%, 97% ee
5j, 61%, 96% ee
5k, 72%, 95% ee
5l, 61%, 88% ee
5m, 63%, 96% ee
5n, 68%, 98% ee
5o, 63%, 96% ee
5p,, 51%, dr > 20:1

Figure 2. Substrate scopes. a) Substrate scope of aryl bromides. b) Substrate scope of amino acid derivatives.

indole, pyrazole, and oxazole, along with other related units, were excellent reaction partners for this transformation. These reactions yielded products **4v**-**4af** in yields ranging from 61% to 81%, accompanied by ee values between 92% and 98%. Besides these, two aryl bromides bearing chiral side chains were employed as reactants to react with butadiene **2a** and amino acid ester **3a**; products **4ag** and **4ah** were generated in good yields and excellent diastereoselectivities. However, the alkyl bromides could not participate in this reaction. For example, desired product **4ai** was not observed when we used bromocyclohexane as the reactant.

https://doi.org/10.1021/acscatal.5c02967
ACS Catal. 2025, 15, 15734−15744

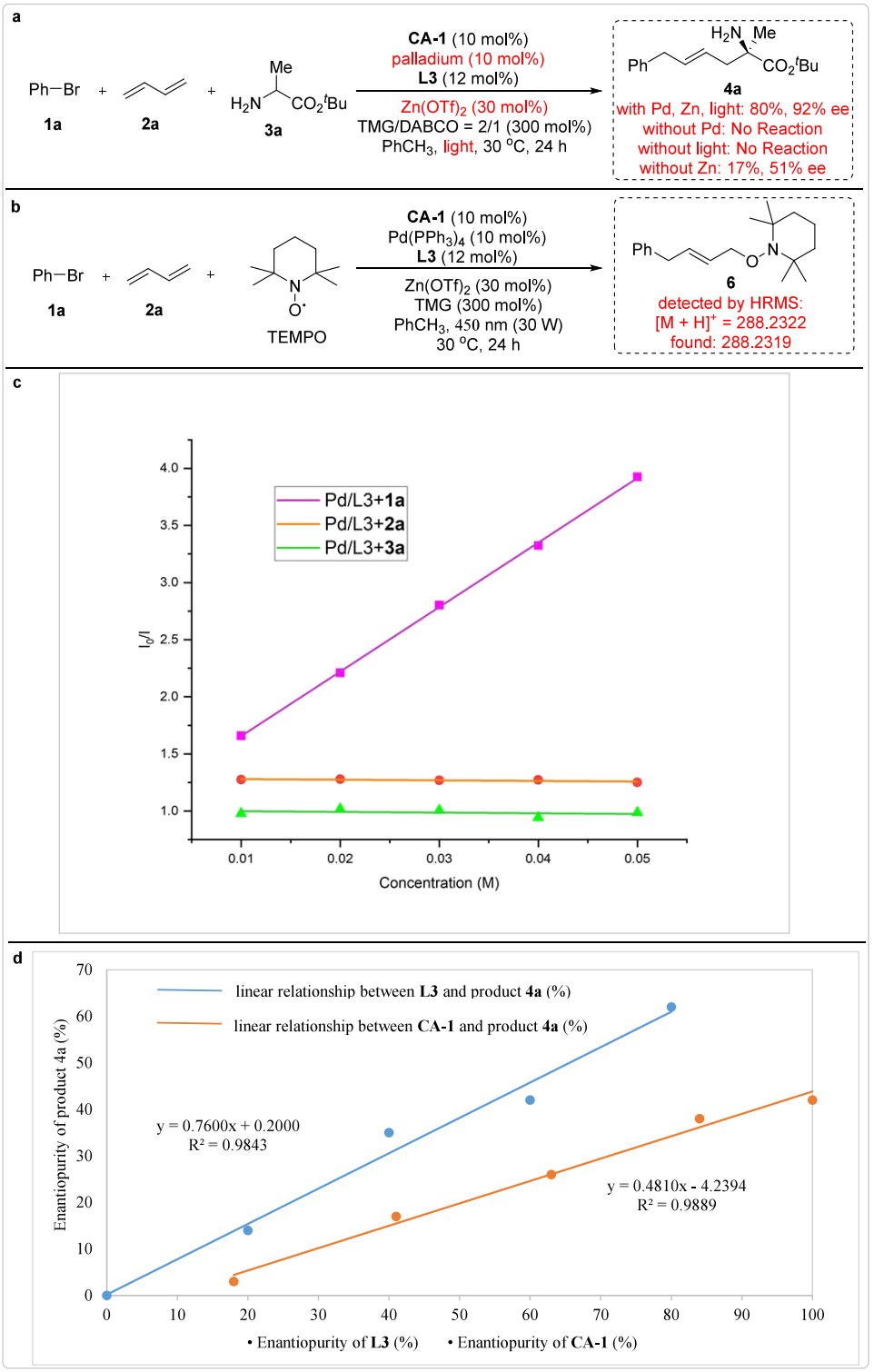

Figure 3. Mechanism investigations were carried out by control experiments. a) Control experiments. b) Intermediate trapping. c) Stern−Volmer fluorescence quenching experiments. d) Nonlinear effect investigations.

Subsequently, various substituted amino acid esters were utilized as donors in this reaction. The results indicated that amino acid esters containing an α-alkyl or alkenyl group served as effective reaction partners for **1a** and **2a**, yielding the desired products **5a**-**5d** with yields ranging from 55% to 79% and ee values between 91% and 98%. Amino acid esters derived from phenyl glycines and phenylalanines also demonstrated favorable reactivity in this reaction, producing products **5e**-**5j** in good yields and enantioselectivities. Additionally, other amino acid esters—including derivatives of serine, aspartic acid, glutamic acid, methionine, and lysine, reacted smoothly with **1a** and **2a**, resulting in products **5k**-**5o** with outstanding experimental outcomes. Notably, the *L*-alanine-derived dipeptide participated effectively in this reaction as well, leading to product **5p** with a yield of 51% while exhibiting excellent diastereoselectivity (>20:1). This finding provides a promising

https://doi.org/10.1021/acscatal.5c02967
ACS Catal. 2025, 15, 15734−15744

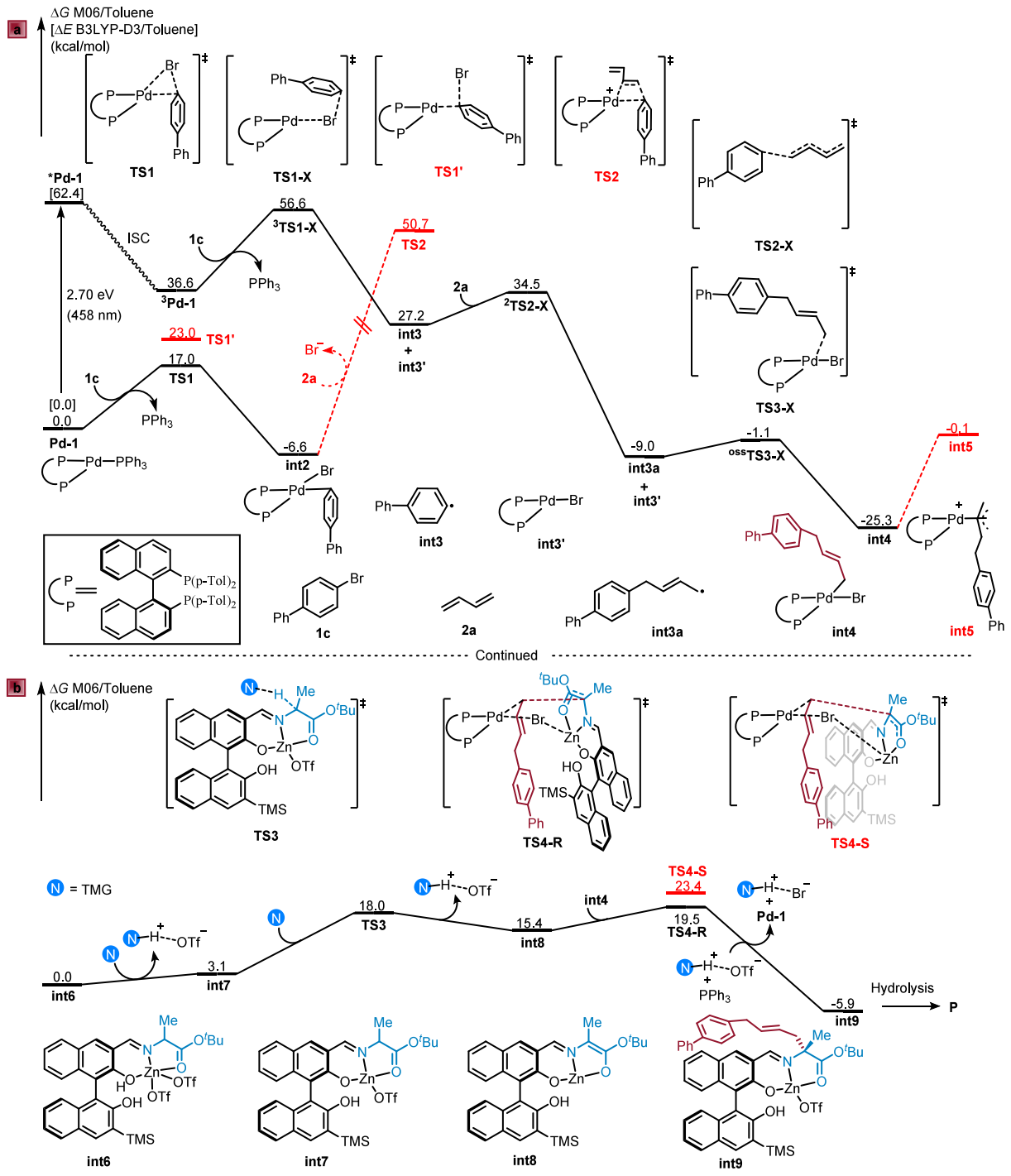

Figure 4. Relative Gibbs free energy profiles for the reaction in the M06/6−311+G(d,p)(SDD for Pd, Zn, and Br)/SMD(Toluene)//B3LYP-D3/6−31G(d)(SDD for Pd, Zn, and Br) level. The energy values in square brackets are in kcal/mol and represent the electronic energy calculated at the B3LYP-D3/6−311+G(d,p)(SDD for Pd)/SMD(Toluene) level of theory in toluene solvent. a) Relative Gibbs free energy profiles for palladium catalysis. b) Relative Gibbs free energy profiles for chiral aldehyde catalysis.

perspective for the postmodification of peptides using this method.

Control Experiments. To elucidate the possible reaction mechanism of this process, several control experiments were conducted. First, the reaction was performed in the absence of palladium, zinc salt, and light irradiation. Under these specific control conditions, the reaction outcomes varied greatly, indicating that all of light, Lewis acid and palladium are essential for this transformation (Figure 3a). Subsequently, under optimal reaction conditions, amino acid ester **3a** was substituted with the radical capture agent TEMPO. The formation of product **6** confirmed that this reaction proceeds via a light-induced radical pathway (Figure 3b). To identify which species were excited by the light, UV/vis characterization of reactants **1a**, **2a**, and **3a**, the palladium source and ligand **L3**, and the corresponding Pd-**L3** complex were carried out (see Supporting Information). The results demonstrated that only palladium and the Pd-**L3** complex exhibited UV

https://doi.org/10.1021/acscatal.5c02967
ACS Catal. 2025, 15, 15734−15744

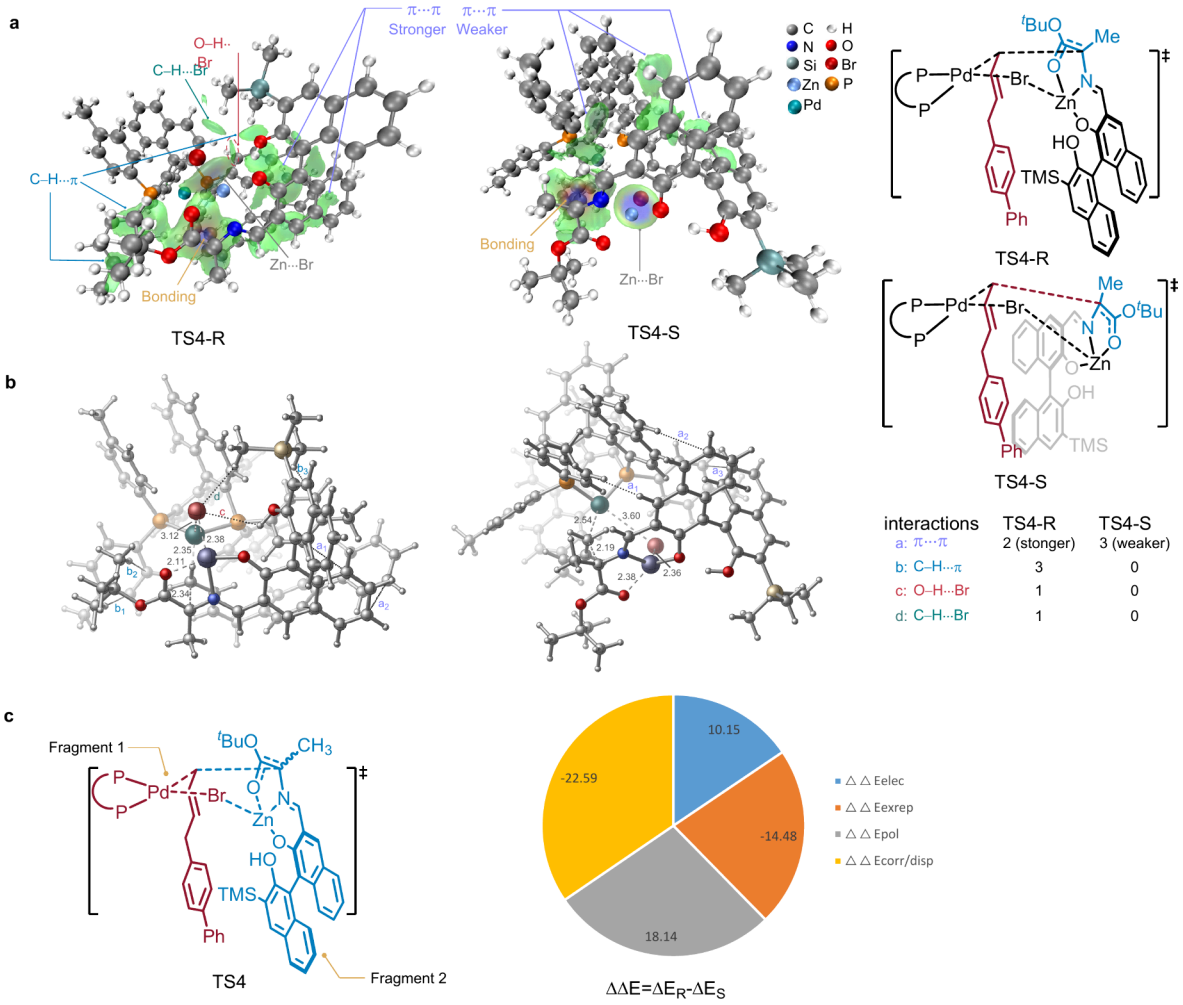

Figure 5. Origin of enantioselectivity. a) IGMH analysis of the noncovalent interactions in **TS4**. b) Illustration of the numbers of major noncovalent interactions in enantiomers of **TS4**. c) Energy decomposition analysis based on XEDA program in **TS4**. All energies are in kcal/mol.

absorbance between 400 and 600 nm. This suggests that a Pd-excitation pathway is involved in this reaction. Furthermore, Stern−Volmer fluorescence quenching experiments were conducted to determine which reactant directly interacts with the excited palladium species. We found that only phenyl bromide **1a** could effectively quench the excited palladium catalyst (Figure 3c). Therefore, it is reasonable to deduce that this reaction initiates with the generation of phenyl radicals, facilitated by photoinduced palladium catalysis. In addition to these investigations, nonlinear effect studies were respectively performed on chiral aldehyde catalyst **CA-1** and chiral ligand **L3**. The observed linear relationships between the ee values of product **4a** and **CA-1** or **L3** indicate that both **CA-1** and **L3** provides only one molecule to participate in the formation of transition states (Figure 3d).

DFT Calculations. To further understand the reaction mechanism, especially for the generation of enantioselectivity, DFT calculations were adopted to investigate possible reaction pathways. As shown in Figure 4(a), on the one hand, computational studies suggest that the reaction is unlikely to occur via the ground state pathway since the high energy barrier of the insertion transition state **TS2** is 57.3 kcal/mol, although oxidative addition transition state **TS1** of aryl bromides **1c** to Pd(0) species is more reasonable with barrier of 17.0 kcal/mol than the S_NAr type transition state **TS1′** whose barrier is 23.0 kcal/mol. On the other hand, under irradiation Pd(0) species could be excited to excited states ***Pd-1** with the 2.70 eV energy gap which corresponds to a λ_{max} of 458 nm. This excited state could decay to triplet states ^{3}**Pd-1** through intersystem crossing (ISC). Immediately, ^{3}**Pd-1** undergoes a halogen atom transfer with aryl bromides **1c** to generate the aryl radical **int3** and LPd(I)Br. Aryl radical **int3** rapidly adds to butadiene to produce allylic radical **int3a** via transition state ^{2}**TS2-X** with an energy barrier of 7.3 kcal/mol. Allylic radical **int3a** then collapses with LPd(I)Br to form η^1-allyl-Pd(II) **int4** which participates in the subsequent enantioselectivity-determining step as an active intermediate, while we also found that η^1-allyl-Pd(II) **int4** is thermodynamically unfavorable to form η^3-π-allyl-Pd(II) species **int5** ($\triangle G$ = 25.2 kcal/mol). Meanwhile, as shown in Figure 4(b), in the **CA**-catalyzed cycle, **int6** will process twice deprotonation using TMG base via transition state **TS3**, leading to the other active intermediate **int8** which collaborates with η^1-allyl-Pd(II) **int4** to participate in the enantioselectivity-determining step via transition state **TS4-R** and **TS4-S** in order to promote C−C bond formation. The computational results indicate that the relative free energy of **TS4-R** is 3.9 kcal/mol lower than that of **TS4-S**. Finally, the hydrolysis of intermediate **int9** yields the target product.

https://doi.org/10.1021/acscatal.5c02967
ACS Catal. 2025, 15, 15734−15744

Scheme 1. Synthetic Applications. a) Scale-up Experiment. b) Product Derivation via Suzuki-Coupling. c) Product Derivation via Sonogashira-Coupling. d) Product Derivation via Bifunctionalization of the Alkene Unit. e) Asymmetric Synthesis of α-Me-L-Lysine Derivative

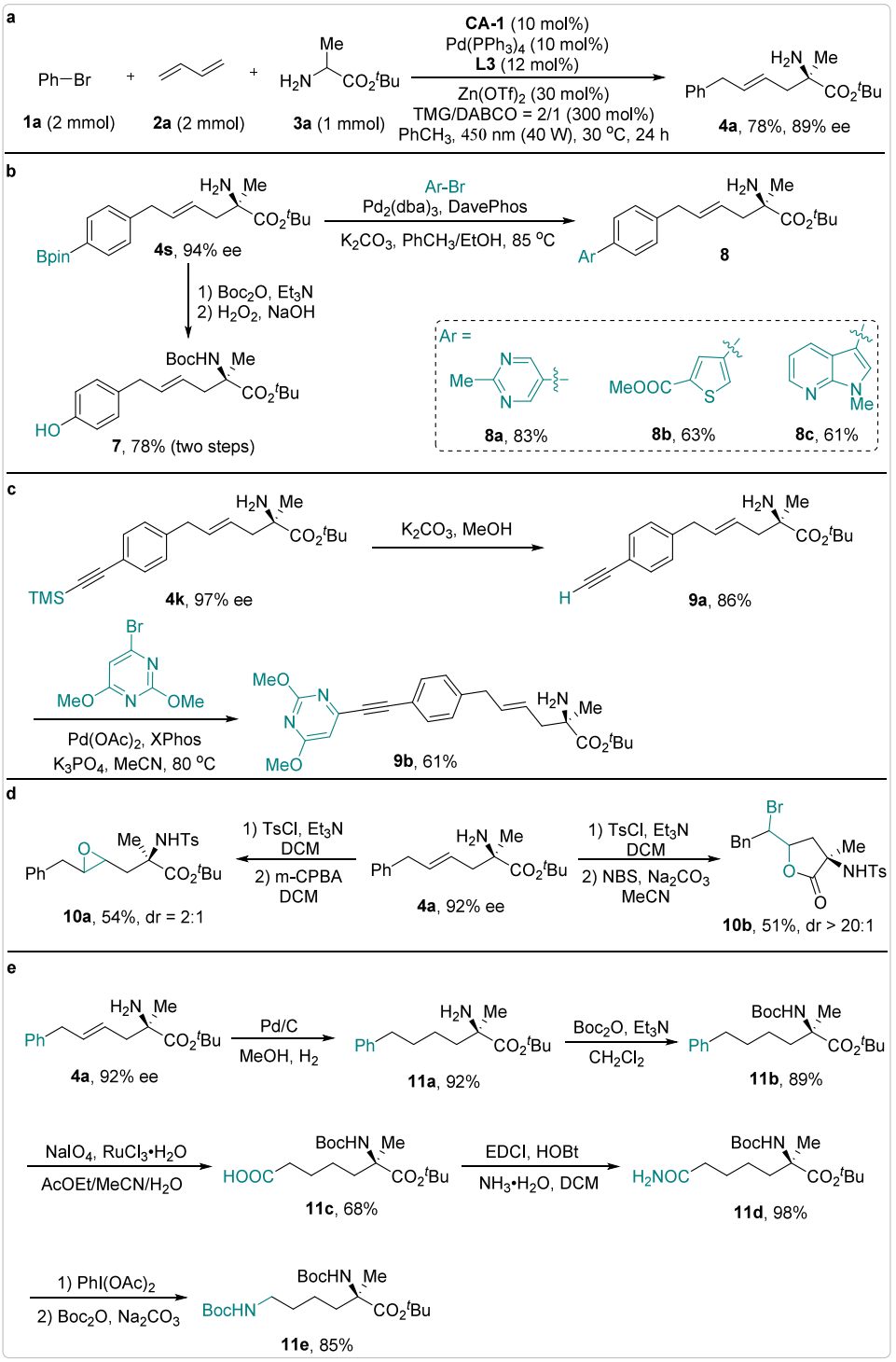

To delve deeper into the origin of enantioselectivity, the independent gradient model based on Hirshfeld partition (IGMH)[51] was used to study the noncovalent interactions between the η^1-allyl-Pd(II) **int4** fragment and the chiral aldehyde (**CA**) fragment **int9** in both **TS4-R** and **TS4-S**. Various interactions between Pd and Zn fragments are visualized in Figure 5a and the numbers of interaction pairs are tabulated in Figure 5b. A wider green surface among the ligand, **CA**, and aryl substrate, which represents a stronger $\pi\cdots\pi$ interaction, is observed in **TS4-R** compared to **TS4-S**. Moreover, four pairs of C−H···X (X = Br, π) and one pair of O−H···Br interactions exist in **TS4-R** that does not exist in **TS4-S** (see below, Figure 5a). Therefore, the large number of these dispersion forces from the ligand and **CA** prove indispensable to the excellent level of enantiocontrol (see below, Figure 5b).

https://doi.org/10.1021/acscatal.5c02967
ACS Catal. 2025, 15, 15734−15744

Furthermore, energy decomposition analysis based on XEDA program[52,53] was conducted to quantitatively evaluate the effect of different ligand−substrate interactions on the enantioselectivity. Comparison of the EDA results between **TS4-R** and **TS4-S** reveals that the more stabilizing dispersion interaction in **TS4-R** is the dominant factor controlling the enantioselectivity (Figure 5c). On the basis of previous studies exploring the nature of weak interactions, C−H···X interactions are claimed to be mainly from dispersion and electrostatic effect,[54] while $\pi\cdots\pi$ stacking is mainly a dispersion interaction.[55,56] Thus, the XEDA results provide a quantitative complement for the qualitative IGMH analysis. Collectively, they clarify that in this reaction the dispersion interaction including the stronger C−H···X and $\pi\cdots\pi$ interactions, primarily between the ligand and **CA**, plays a dominant role in the enantiocontrol which corresponds to the results of nonlinear effect studies indicating the chirality affected by the ligand and **CA** collaboratively.

Synthetic Applications. To illustrate the potential synthetic values, a scale-up experiment and several product derivations were carried out. Results indicate that this reaction could produce compound **4a** with 78% yield and 89% ee at a 1 mmol scale (Scheme 1a). The excellent functional group tolerance of this reaction facilitates the synthesis of structurally complex chiral molecules from the corresponding catalytic products. For instance, product **4s** can be transformed into other chiral compounds through oxidation or coupling reactions, yielding amino acid esters **7** and **8a**-**8c** in good yields (Scheme 1b). Following the removal of the trimethylsilyl group from compound **4k**, a Sonogashira coupling reaction can occur between **9a** and 4-bromo-2,6-dimethoxypyrimidine, resulting in the formation of pyrimidyl-containing amino acid ester **9b** with satisfactory yields (Scheme 1c). Moreover, various functional group transformations can also be performed on the alkene units present in the catalytic products. For example, amino acid ester **10a** featuring an epoxy group was synthesized by treating compound **4a** with *m*-CPBA (*m*-chloroperoxybenzoic acid). Additionally, bromine-containing α-amino lactone **10b** was produced via a tandem bromination/lactonization reaction starting from compound **4a** (Scheme 1d). Most importantly, one derivative of chiral α-methyl lysines—widely utilized in drug molecule or peptide synthesis[57]—can be readily prepared from compound **4a**. Through five commonly employed chemical transformations, compound **11e** was generated with an overall yield of 46% (Scheme 1e). This represents a highly efficient pathway for producing chiral α-methyl lysine derivatives based on asymmetric catalysis.

CONCLUSION

In conclusion, under light irritation, a chiral aldehyde/palladium cocatalysis has enabled the efficient asymmetric 1,4-arylalkylation of petrochemical butadiene. A diverse range of optically active α,α-disubstituted α-amino acid esters are generated with good to excellent yields and enantioselectivities. The detailed reaction mechanism elucidating the observed chemoselectivity, regioselectivity, and enantioselectivity in this transformation has been meticulously investigated. Notably, a novel reaction model for chiral aldehyde/palladium catalysis is given by DFT calculations. Furthermore, a series of functional group transformations have been performed to construct structurally diverse chiral molecules and valuable nonproteinogenic amino acid derivatives featuring tertiary α-chiral carbon centers.

EXPERIMENTAL SECTION

All information regarding the materials and methods used in this work is listed in the Supporting Information.

General Procedure for the Catalytic Asymmetric Reaction. Under nitrogen atmosphere, an oven-dried 10 mL Schlenk tube containing a magnetic stir bar was charged with $[Pd(PPh_3)_4]$ (23.1 mg, 0.02 mmol), **L3** (16.3 mg, 0.024 mmol), chiral aldehyde **CA-1** (7.7 mg, 0.02 mmol), $Zn(OTf)_2$ (21.8 mg, 0.06 mmol), DABCO (0.2 mmol), and toluene (0.5 mL). Subsequently, aryl bromides **1** (0.4 mmol), butadiene **2a** (0.4 mmol, 20 wt % in toluene), amino acid ester **3** (0.2 mmol), and TMG (50.1 uL, 0.4 mmol) were successively added. The reaction mixture was stirred at 30 °C for 24 h under blue LEDs irradiation (40 W). After the reaction was completed, the solvent was removed by rotary evaporation, and the residue was purified by flash silica gel column chromatography separation with petroleum/ethyl acetate as the eluent to afford products **4** or **5**.

ASSOCIATED CONTENT

Supporting Information

The Supporting Information is available free of charge at https://pubs.acs.org/doi/10.1021/acscatal.5c02967.

Experimental procedures, compound characterization data, and ^{1}H NMR, ^{13}C NMR spectral data and HPLC results (PDF)

AUTHOR INFORMATION

Corresponding Authors

Yan-Min Huang − *Guangxi Key Laboratory of Natural Polymer Chemistry and Physics, Nanning Normal University, Nanning 530001, China*; Email: huangyanmin828@gxtc.edu.com

Yu Lan − *School of Chemistry and Chemical Engineering, Chongqing Key Laboratory of Theoretical and Computational Chemistry, Chongqing University, Chongqing 400030, China*; orcid.org/0000-0002-2328-0020; Email: lanyu@cqu.edu.cn

Qi-Xiang Guo − *Key Laboratory of Applied Chemistry of Chongqing Municipality, and Chongqing Key Laboratory of Soft-Matter Material Chemistry and Function Manufacturing, School of Chemistry and Chemical Engineering, Southwest University, Chongqing 400715, China*; orcid.org/0000-0002-0405-7958; Email: qxguo@swu.edu.cn

Authors

Jian-Hua Liu − *Key Laboratory of Applied Chemistry of Chongqing Municipality, and Chongqing Key Laboratory of Soft-Matter Material Chemistry and Function Manufacturing, School of Chemistry and Chemical Engineering, Southwest University, Chongqing 400715, China*

Lei Xu − *School of Chemistry and Chemical Engineering, Chongqing Key Laboratory of Theoretical and Computational Chemistry, Chongqing University, Chongqing 400030, China*

Wei Wen − *Key Laboratory of Applied Chemistry of Chongqing Municipality, and Chongqing Key Laboratory of*

https://doi.org/10.1021/acscatal.5c02967
ACS Catal. 2025, 15, 15734−15744

Soft-Matter Material Chemistry and Function Manufacturing, School of Chemistry and Chemical Engineering, Southwest University, Chongqing 400715, China; orcid.org/0000-0001-5100-8545

Zhu-Lian Wu − *Key Laboratory of Applied Chemistry of Chongqing Municipality, and Chongqing Key Laboratory of Soft-Matter Material Chemistry and Function Manufacturing, School of Chemistry and Chemical Engineering, Southwest University, Chongqing 400715, China*

Tian Cai − *Key Laboratory of Applied Chemistry of Chongqing Municipality, and Chongqing Key Laboratory of Soft-Matter Material Chemistry and Function Manufacturing, School of Chemistry and Chemical Engineering, Southwest University, Chongqing 400715, China*

Complete contact information is available at: https://pubs.acs.org/10.1021/acscatal.5c02967

Author Contributions

⊥These authors contributed equally

Notes

The authors declare no competing financial interest.

■ ACKNOWLEDGMENTS

We are grateful for financial support from NSFC (22371233, 22071199), and the Innovation Research 2035 Pilot Plan of Southwest University (SWU-XDZD22011).

■ REFERENCES

(1) Wang, P.-Z.; Xiao, W.-J.; Chen, J.-R. Recent advances in radical mediated transformations of 1,3-dienes. *Chin. J. Catal.* **2022**, *43*, 548−557.

(2) Huang, Y.; Shen, L.; Ma, C.; Jiang, Y.; Yu, B. Functionalization of 1,3-butadiene derivatives under photo/electrocatalysis. *Eur. J. Org. Chem.* **2024**, *27*, No. e202400403.

(3) Iwasaki, T. Catalytic functionalization of 1,3-butadiene by carbon electrophiles. *J. Jpn. Petrol. Inst.* **2020**, *63*, 123−132.

(4) Yang, J.; Wang, P.; Neumann, H.; Jackstell, R.; Beller, M. Industrially applied and relevant transformations of 1,3-butadiene using homogeneous catalysts. *Ind. Chem. Mater.* **2023**, *1*, 155−174.

(5) Thiele, S. K. H.; Wilson, D. R. Alternate transition metal complex based diene polymerization. *J. Macromol. Sci., Part C: Polym. Rev.* **2003**, *43*, 581−628.

(6) Richards, D. H. The polymerization and copolymerization of butadiene. *Chem. Soc. Rev.* **1977**, *6*, 235−260.

(7) Furukawa, J. Stereoregular and sequence-regular polymerization of butadiene. *Acc. Chem. Res.* **1980**, *13*, 1−6.

(8) Tobisch, S. Theoretical investigation of the mechanism of cis-trans regulation for the allylnickel(II)-catalyzed 1,4 polymerization of butadiene. *Acc. Chem. Res.* **2002**, *35*, 96−104.

(9) Tang, S.; et al. Sustainable copolymer synthesis from carbon dioxide and butadiene. *Chem. Rev.* **2024**, *124*, 3590−3607.

(10) Perry, G. J. P.; Jia, T.; Procter, D. J. Copper-catalyzed functionalization of 1,3-dienes: hydrofunctionalization, borofunctionalization, and difunctionalization. *ACS Catal.* **2020**, *10*, 1485−1499.

(11) McNeill, E.; Ritter, T. 1,4-Functionalization of 1,3-dienes with low-valent iron catalysts. *Acc. Chem. Res.* **2015**, *48*, 2330−2343.

(12) Xiong, Y.; Sun, Y.; Zhang, G. Recent advances on catalytic asymmetric difunctionalization of 1,3-dienes. *Tetrahedron Lett.* **2018**, *59*, 347−355.

(13) Wu, X.; Gong, L.-Z. Palladium (0)-catalyzed difunctionalization of 1,3-dienes: from racemic to enantioselective. *Synthesis* **2019**, *51*, 122−134.

(14) Huang, H.-M.; Bellotti, P.; Pfluger, P. M.; Schwarz, J. L.; Heidrich, B.; Glorius, F. Three-component, interrupted radical Heck/allylic substitution cascade involving unactivated alkyl bromides. *J. Am. Chem. Soc.* **2020**, *142*, 10173−10183.

(15) Li, Y.-L.; Li, W.-D.; Gu, Z.-Y.; Chen, J.; Xia, J.-B. Photoredox Ni-catalyzed branch-selective reductive coupling of aldehydes with 1,3-dienes. *ACS Catal.* **2020**, *10*, 1528−1534.

(16) Schwarz, J. L.; Huang, H.-M.; Paulisch, T. O.; Glorius, F. Dialkylation of 1,3-dienes by dual photoredox and chromium catalysis. *ACS Catal.* **2020**, *10*, 1621−1627.

(17) Ding, D.; Fan, L.-F.; Han, Z.-Y.; Wang, P.-S. Redox-neutral 1,4-dicarbonfunctionalization of 1,3-butadiene by merging photoredox and nickel catalysis. *Org. Lett.* **2023**, *25*, 210−214.

(18) Li, F.; Lin, S. J.; Chen, Y. Q.; Shi, C. Z.; Yan, H. P.; Li, C. C.; Wu, C.; Lin, L. Q.; Duan, C. Y.; Shi, L. Photocatalytic generation of π-allyltitanium complexes via radical intermediates. *Angew. Chem., Int. Ed.* **2021**, *60*, 1561−1566.

(19) Song, S.; Yin, Y.-Z.; Han, Z.-Y. A photoinduced palladium-catalyzed cascade reaction for the synthesis of chiral piperidines with chiral amino acid derivatives and 1,3-dienes. *Synthesis* **2023**, *55*, 3793−3798.

(20) Shi, Y.; Zhang, Z.-S.; Shao, J.; Fu, C.; Xiong, L.-T.; Li, Z.-D.; Cui, Z.-N. Photoinduced palladium-catalyzed 1,3-diene-selective fluoroalkylamination compounds as potential bactericidal agent against Xanthomonas oryzae pv. *Oryzae. Chin. Chem. Lett.* **2024**, *35*, No. 108794.

(21) Cheung, K. P. S.; Kurandina, D.; Yata, T.; Gevorgyan, V. Photoinduced Palladium-Catalyzed Carbofunctionalization of Conjugated Dienes Proceeding via Radical-Polar Crossover Scenario: 1,2-Aminoalkylation and Beyond. *J. Am. Chem. Soc.* **2020**, *142*, 9932−9937.

(22) Huang, H. M.; Koy, M.; Serrano, E.; Pfluger, P. M.; Schwarz, J. L.; Glorius, F. Catalytic radical generation of π-allylpalladium complexes. *Nat. Catal.* **2020**, *3*, 393−400.

(23) Zbieg, J. R.; Yamaguchi, E.; McInturff, E. L.; Krische, M. J. Enantioselective C-H crotylation of primary alcohols via hydrohydroxyalkylation of butadiene. *Science* **2012**, *336*, 324−327.

(24) Li, C.; Liu, R. Y.; Jesikiewicz, L. T.; Yang, Y.; Liu, P.; Buchwald, S. L. CuH-Catalyzed enantioselective ketone allylation with 1,3-dienes: scope, mechanism, and applications. *J. Am. Chem. Soc.* **2019**, *141*, 5062−5070.

(25) Wang, Y.; Zhang, J.; You, C.; Mi, X.; Luo, S. Z. Catalytic asymmetric addition and telomerization of butadiene with enamine intermediates. *CCS Chem.* **2022**, *4*, 2267−2275.

(26) Yu, H.; Zhang, Q.; Zi, W. Enantioselective three-component photochemical 1,4-bisalkylation of 1,3-butadiene with Pd/Cu catalysis. *Angew. Chem., Int. Ed.* **2022**, *61*, No. e202208411.

(27) Xiong, Y.; Zhang, G. Enantioselective 1,2-difunctionalization of 1,3-butadiene by sequential alkylation and carbonyl allylation. *J. Am. Chem. Soc.* **2018**, *140*, 2735−2738.

(28) Tang, S.-Y.; Wang, Z.-J.; Ao, Y.; Wang, N.; Huang, H.-M. Photoredox/Cr-catalyzed enantioselective radical-polar crossover transformation via C-H functionalization. *Nat. Commun.* **2025**, *16*, 1354.

(29) Zhan, X. H.; Nie, Z. W.; Li, N.; Zhou, A.; Lv, H. T.; Liang, M. R.; Wu, K. Q.; Cheng, G. J.; Yin, Q. Catalytic asymmetric cascade dearomatization of indoles via a photoinduced Pd-catalyzed 1,2-bisfunctionalization of butadienes. *Angew. Chem., Int. Ed.* **2024**, *63*, No. e202404388.

(30) Li, Y.; Zhang, L. M.; Li, X. T.; Liu, H.; Song, T. T.; Ji, D. W.; Chen, Q. A. Stereoselective 1,3-cyclotelomerization of butadiene with dienophiles under nickel catalysis. *J. Am. Chem. Soc.* **2025**, *147*, 19421−19431.

(31) Pratsch, G.; Heinrich, M. R. Modern Developments in Aryl Radical Chemistry. In *Radicals in Synthesis III*; Heinrich, M., Gansäuer, A., Eds.; Topics in Current Chemistry, Vol. *320*; Springer, 2011.

(32) Waldvogel, S. R.; Lips, S.; Selt, M.; Riehl, B.; Kampf, C. J. Electrochemical arylation reaction. *Chem. Rev.* **2018**, *118*, 6706−6765.
(33) Ghosh, T.; Santra, S.; Zyryanov, G. V.; Ranu, B. C. Recent advances in visible light mediated photoinduced aryl radical generation and its application in synthesis. *J. Photochem. Photobiol.* **2023**, *16*, No. 100192.
(34) Bugaenko, D. I.; Volkov, A. A.; Karchava, A. V.; Yurovskaya, M. A. Generation of aryl radicals by redox processes. Recent progress in the arylation methodology. *Russ. Chem. Rev.* **2021**, *90*, 116−170.
(35) Ghosh, I.; Marzo, L.; Das, A.; Shaikh, R.; König, B. Visible light mediated photoredox catalytic arylation reactions. *Acc. Chem. Res.* **2016**, *49*, 1566−1577.
(36) Ye, Z.; Ma, W.; Zhang, X.; Liu, H.; Zhang, F. Electrochemically driven nickel-catalyzed enantioselective hydro-arylation/alkenylation of enones. *Adv. Sci.* **2024**, *11*, No. 2405926.
(37) Cai, Y.; Gaurav, G.; Ritter, T. 1,4-Aminoarylation of butadienes via photoinduced palladium catalysis. *Angew. Chem., Int. Ed.* **2024**, *63*, No. e202311250.
(38) Chen, L.; Luo, M.-J.; Zhu, F.; Wen, W.; Guo, Q.-X. Combining chiral aldehyde catalysis and transition-metal catalysis for enantioselective α-allylic alkylation of amino acid esters. *J. Am. Chem. Soc.* **2019**, *141*, 5159−5163.
(39) Liu, J.-H.; Zhou, Q.; Lin, Y.; Wu, Z. L.; Cai, T.; Wen, W.; Huang, Y. M.; Guo, Q. X. Modular chiral-aldehyde/palladium catalysis enables atom-economical α-allylation of *N*-unprotected amino acid esters with 1,3-dienes and allenes. *ACS Catal.* **2023**, *13*, 6013−6022.
(40) Zhou, Q.; Yin, Z. W.; Wu, Z. L.; Cai, T.; Wen, W.; Huang, Y. M.; Guo, Q. X. Asymmetric α-allylation of *N*-unprotected amino acid esters with 1,3-disubstituted allyl acetates enabled by chiral-aldehyde/palladium catalysis. *Org. Lett.* **2023**, *25*, 5790−5794.
(41) Liu, J.-H.; Wen, W.; Wu, Z. L.; Cai, T.; Huang, Y. M.; Guo, Q. X. Asymmetric three-component Tsuji−Trost allylation reaction enabled by chiral aldehyde/palladium combined catalysis. *Chem. Sci.* **2024**, *15*, 10232−10236.
(42) Han, H.; Yi, W.; Ding, S.; Ren, X.; Zhao, B. Enantioselective three-component α-allylic alkylation of α-amino esters by synergistic photoinduced Pd/carbonyl catalysis. *Angew. Chem., Int. Ed.* **2025**, *64*, No. e202418910.
(43) Chang, X.; Cheng, X.; Liu, X. T.; Fu, C.; Wang, W. Y.; Wang, C. J. Stereodivergent construction of 1,4-nonadjacent stereocenters via hydroalkylation of racemic allylic alcohols enabled by copper/ruthenium relay catalysis. *Angew. Chem., Int. Ed.* **2022**, *61*, No. e202206517.
(44) Wang, H.; Zhang, R.; Zi, W. Synergistic palladium/copper-catalyzed 1,4-difunctionalization of 1,3-dienes for stereodivergent construction of 1,5-nonadjacent stereocenters. *Angew. Chem., Int. Ed.* **2024**, *63*, No. e202402843.
(45) Li, P.; Liu, Z.; Huo, X.; Zhang, W. Stereodivergent construction of 1,5/1,7-nonadjacent tetrasubstituted stereocenters enabled by Pd/Cu-cocatalyzed asymmetric Heck cascade reaction. *Angew. Chem., Int. Ed.* **2024**, *63*, No. e202407498.
(46) Huo, X.; Li, G.; Wang, X.; Zhang, W. Bimetallic catalysis in stereodivergent synthesis. *Angew. Chem., Int. Ed.* **2022**, *61*, No. e202210086.
(47) Wei, L.; Fu, C.; Wang, Z.-F.; Tao, H.-Y.; Wang, C.-J. Synergistic dual catalysis in stereodivergent synthesis. *ACS Catal.* **2024**, *14*, 3812−3844.
(48) Lee, S.; Beare, N. A.; Hartwig, J. F. Palladium-catalyzed α-arylation of esters and protected amino acids. *J. Am. Chem. Soc.* **2001**, *123*, 8410−8411.
(49) Ma, F.; Xie, X.; Ding, L.; Gao, J.; Zhang, Z. Palladium-catalyzed coupling reaction of amino acids (esters) with aryl bromides and chlorides. *Tetrahedron* **2011**, *67*, 9405−9410.
(50) Albat, D.; Neudoerfl, J. M.; Schmalz, H. G. A general stereocontrolled synthesis of opines through asymmetric Pd-catalyzed N-allylation of amino acid esters. *Eur. J. Org. Chem.* **2021**, *2021*, 2099−2102.
(51) Lu, T.; Chen, Q. Independent gradient model based on Hirshfeld partition: A new method for visual study of interactions in chemical systems. *J. Comput. Chem.* **2022**, *43*, 539−555.
(52) Su, P.; Tang, Z.; Wu, W. Generalized Kohn-Sham energy decomposition analysis and its applications. *WIREs Comput. Mol. Sci.* **2020**, *10*, No. e1460.
(53) Tang, Z.; Song, Y. L.; Zhang, S.; Wang, W.; Xu, Y.; Wu, D.; Wu, W.; Su, P. F. XEDA, a fast and multipurpose energy decomposition analysis program. *J. Comput. Chem.* **2021**, *42*, 2341−2351.
(54) Emamian, S.; Lu, T.; Kruse, H.; Emamian, H. Exploring nature and predicting strength of hydrogen bonds: a correlation analysis between atoms-in-molecules descriptors, binding energies, and energy components of symmetry-adapted perturbation theory. *J. Comput. Chem.* **2019**, *40*, 2868−2881.
(55) Tsuzuki, S.; Honda, K.; Uchimaru, T.; Mikami, M.; Tanabe, K. Origin of attraction and directionality of the π/π interaction: model chemistry calculations of benzene dimer interaction. *J. Am. Chem. Soc.* **2002**, *124*, 104−112.
(56) Carter-Fenk, K.; Herbert, J. M. Electrostatics does not dictate the slip-stacked arrangement of aromatic $\pi-\pi$ interactions. *Chem. Sci.* **2020**, *11*, 6758−6765.
(57) Chauhan, S. S. Enantioselective synthesis of (L)-Fmoc-a-Me-Lys(Boc)-OH via diastereoselective alkylation of oxazinone as a chiral auxiliary. *Tetrahedron Lett.* **2009**, *50*, 6913−6915.

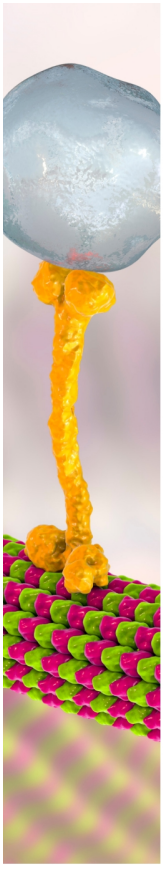
CAS BIOFINDER DISCOVERY PLATFORM™
BRIDGE BIOLOGY AND CHEMISTRY FOR FASTER ANSWERS
Analyze target relationships, compound effects, and disease pathways
Explore the platform
CAS
A division of the American Chemical Society

https://doi.org/10.1021/acscatal.5c02967
ACS Catal. 2025, 15, 15734−15744